Volume 1 | Number 1 | Jan 2013 | Pages 1–100

Journal of
Materials Chemistry A

Materials for energy and sustainability
www.rsc.org/materialsA

Li⁺

ROYAL SOCIETY
OF CHEMISTRY

ROYAL SOCIETY
OF CHEMISTRY

www.rsc.org/materialsA

Amorphous niobium-phosphorus-silicon mixed oxide gels in which the phosphorus results stably bonded to siloxane matrix by niobium bridges have been obtained by a new hydrolytic sol-gel route.

ROYAL SOCIETY
OF CHEMISTRY
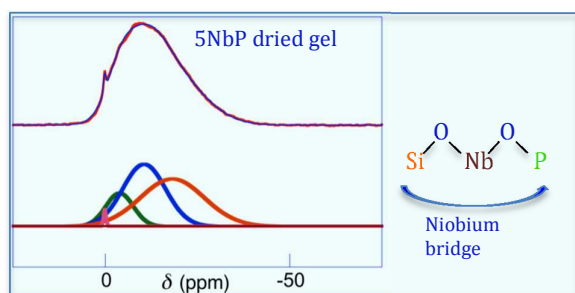
Journal Name

ARTICLE

Phosphorus stably bonded to silica gel matrix through niobium bridges

N. J. Clayden[a], G. Accardo[b], P. Mazzei[c], A. Piccolo[d c], P. Pernice[e c], A. Vergara[f], C. Ferone[b] and A. Aronne[*e c]

For the first time niobium-phosphorus-silicon mixed oxide gels xNb$_2$O$_5$·xP$_2$O$_5$·(100-2x)·SiO$_2$, with x = 2.5 (2.5PNb), 5 (5PNb), 7.5 (7.5PNb) and 10 (10PNb), were synthesized at room temperature by an innovative sol-gel route from phosphoryl chloride, niobium chloride and tetraethoxysilane. Thermogravimetry/differential thermal analysis, X-ray diffraction, solid state ^{29}Si and ^{31}P NMR, Raman and Fourier transform infrared spectroscopy were used to examine the structure of dried and heat-treated (1h at 500 °C) gels. The synthesis procedure tuned in this work allowed obtaining, for each studied composition, transparent chemical gels by means of a careful control of the precursors reactivity. Amorphous dried gels were obtained which were characterized by a very high degree of silicon cross-linking. Moreover, Si—O—Nb bridges were formed which allowed the phosphorus to be anchored stably through Nb—O—P bonds within the gel. All heat-treated gels keep their amorphous nature with high OH groups content, that are mainly linked to phosphorus, make them strong acidic solid.

Introduction

The sol-gel synthesis of mixed oxide materials containing SiO$_2$ and P$_2$O$_5$ has recently attracted great attention as a consequence of their functional properties. In fact, these materials find applications as proton exchange membrane in fuel cells,[1-5] bioactive materials[6-9] and exhibit very interesting surface acidic properties, making them very attractive as solid acid catalysts.[10] Diverse protonic conduction abilities as well as Brønsted acid site distributions were found in these materials as a consequence of the variation in the Si/P molar ratio[11] and the preparation procedure[10] altering the distribution of P-species in the siloxane network.

Although the hydrolytic sol-gel chemistry of phosphosilicates

[a.] School of Chemistry, University of East Anglia, Norwich, NR4 7TJ (UK)
[b.] Dipartimento di Ingegneria, Università di Napoli Parthenope, Centro Direzionale - Isola C4 – I-80143 Napoli, (Italy)
[c.] Centro Interdipartimentale di Ricerca sulla Risonanza Magnetica Nucleare per l'Ambiente, l'Agro-Alimentare ed i Nuovi Materiali (CERMANU), Università di Napoli Federico II, Via Università 100, I-80055 Portici (Italy)
[d.] Dipartimento di Agraria, Università di Napoli Federico II, Via Università 100, I-80055 Portici (Italy)
[e.] Dipartimento di Ingegneria Chimica, dei Materiali e della Produzione Industriale, Università di Napoli Federico II, P.le Tecchio 80, I-80125 Napoli (Italy) E-mail: anaronne@unina.it
[f.] Dipartimento di Scienze Chimiche, Università di Napoli Federico II, Via Cinthia, I-80126, Napoli (Italy)

has been extensively studied, their instability towards humidity remains unresolved, especially for materials of a high P content, owing to the high sensitivity of Si—O—P bonds toward hydrolysis. Thus making it very difficult to prepare, at least at low temperature, materials with stable Si—O—P and/or P—O—P links.[10, 12] To overcome this problem either completely non-aqueous/non-hydrolytic sol-gel routes have been explored[13-15] or specific strategies have been adopted for hydrolytic sol-gel routes: (a) the addition of a third component, such as Al$_2$O$_3$ and B$_2$O$_3$, able to form hydrolytically stable bridging bonds between the phosphate and the silicate matrix instead of the unstable Si—O—P bonds;[16] (b) the preparation of hybrid silicate network containing hydrolytically stable Si—C and P—C bonds by phosphorylation with phosphonic acid in a two-steps route.[1, 3] In (b) case, starting from tetraethoxysilane (TEOS) and aminopropyltriethoxysilane, hybrid silica containing primary amino groups was at first obtained, that was subsequently phosphorylated by Kabachnik-Fields reaction;[1] or, starting from TEOS and diethylphosphatoethyltriethoxysilane, organo-alkoxysilane containing phosphonate groups was firstly prepared; in a subsequent step phosphonate groups were converted in phosphonic ones by acidification.[3]

In this work, a new hydrolytic sol-gel route, characterized by the easy manipulation of precursors and wholly performed at room temperature, is proposed in order to prepare hydrolytically stable mixed oxide materials containing Nb$_2$O$_5$, P$_2$O$_5$ and SiO$_2$ in which the stabilization of Si—O—P bonds is realized by the formation of stable Si—O—Nb and Nb—O—P bonds. The addition of niobium not only stabilizes the material against the humidity but gives it unusual surface acidity

properties, due to the presence of both Lewis and Brønsted acid sites, making it suitable for heterogeneous catalysis in many reactions, such as seen for niobiumphosphate in fructose dehydration,[17-19] Friedel-Craft,[20] and alkylation or benzylation of several aromatic compounds.[21] Moreover, the presence of Si gives further possibilities to modulate the acid characteristics of these materials. Recently, mesoporous niobium-phosphate-silicate characterized by Nb/P atomic ratio equal to 0.5 and 1, that showed catalytic activity in the dehydration of glycerol to acrolein, have been prepared by a solvothermal method combined with solvent evaporation.[22] This route involves different steps at temperature higher than room temperature and requires the use of different precursors both for P (orthophosphoric acid, triethylphosphate and diethylphosphatoethyltriethoxysilane) and for Si (tretraethylorthosilicate and diethylphosphatoethyltriethoxysilane) to control the stoichiometry and homogeneity of the final product.[22]

Among the wet chemical synthesis techniques, the strength of the sol–gel method is that it gives very high homogeneity, down to the molecular and/or the nanometre scale, due its bottom-up approach. This is particularly useful for the preparation of mixed-oxides where the sol-gel method allows materials to be made characterized by a very high dispersion of the components in the matrix of the major phase. The sol-gel chemistry of both P_2O_5-SiO_2[1-11] and Nb_2O_5-SiO_2[23-28] binary systems has been extensively studied. In marked contrast, to the best of our knowledge, phosphorus-niobium-silicon mixed-oxides have never been synthesized previously by sol-gel methods. This is mainly due to the intrinsic difficulty of controlling the hydrolysis and polycondensation reactions of the different molecular precursors as they are characterized by very different hydrolysis rates. Silicon alkoxides undergo hydrolysis much slower than the typical Nb and P molecular precursors such as niobium and phosphorus alkoxides, niobium chloride and phosphoryl chloride. On the other hand phosphoric acid esters exhibit an even slower rate of hydrolysis than silicon alkoxides. Consequently, in both binary systems it is very difficult to obtain a high dispersion of P_2O_5 or Nb_2O_5 in the silica matrix when the oxide content exceeds 10 mol%, since self-condensation prevails over cross-condensation producing phase-separated nanodomains of the mixed oxides.[11, 27]

In the present work, amorphous niobium-phosphorus-silicon mixed oxide materials have been synthesized via sol–gel using an innovative procedure based on those previously described for binary P_2O_5-SiO_2[29] and Nb_2O_5-SiO_2[23] systems. Keeping P/Nb molar ratio equal to one, with the Si content ranging from 95 to 80 mol%, four amorphous materials have been prepared. The influence of the synthesis procedure on the structural features of the gel-derived samples has been investigated by TG/DTA analysis, X-ray diffraction (XRD), solid state ^{29}Si and ^{31}P NMR, Raman and Fourier transform infrared (FTIR) spectroscopy with the aim of evaluating both the degree of dispersion of P and Nb within the siloxane matrix and their extent of cross-condensation.

Experimental

Sol-Gel synthesis

Niobium-phosphorus-silicon mixed oxide materials, whose nominal molar compositions can be expressed by the formula $xNb_2O_5 \cdot xP_2O_5 \cdot (100-2x) \cdot SiO_2$, with x = 2.5, 5, 7.5 and 10, were prepared by a sol-gel method using phosphoryl chloride, $POCl_3$ (99%, Aldrich Chemical), niobium chloride, $NbCl_5$ (99%, Gelest), and tetraethoxysilane, $Si(OC_2H_5)_4$ (99%, Gelest), as starting materials. Hereafter the dried gels will be indicated with the x value followed by the symbol of niobium and phosphorus (i.e. 2.5NbP, 5NbP etc) while gels annealed at 500 °C for 1h will be indicated as the dried gels followed by the annealing temperature (i.e. 2.5NbP-500, 5NbP-500, etc.)

The preparation procedure was completely performed at room temperature. The alcoholic solutions of the precursors were prepared and then hydrolyzed in an acidic environment according to the flow-chart procedure showed in Figure 1. A solution of $NbCl_5$ in anhydrous ethanol (EtOH) having the molar ratio $NbCl_5$: EtOH = 1 : 6 was prepared in a dry box and was fluxed with dry-air for 20 min to allow the HCl removal in some extent and the formation of partially substituted $Nb(OEt)_{5-x}(Cl)_x$ species. An alcoholic solution of TEOS with molar ratio TEOS : EtOH = 1 : 4 was stirred for 5 min and then mixed with the first one. Successively, this solution was mixed with a solution previously prepared in a dry box of $POCl_3$ in anhydrous EtOH ($POCl_3$: EtOH = 1 : 6).

The resulting clear solution was hydrolyzed, under stirring, using a hydro-alcoholic solution so to obtain the final molar ratio TEOS : H_2O = 1 : 4 for each composition (Figure 1).

Transparent gels were obtained from this final solution with gelation occurring within 3 days for all samples. The gelled systems were kept for 2 more days at room temperature before drying. The gels were fully dried in air at 110 °C in an electric oven for 3 days. After these heat-treatments, transparent and hardened dry gels were obtained for all compositions that were finely ground to allow the thermal and structural characterization.

Thermal and structural characterization.

The weight loss of the dried gels as well as the nature and temperatures of the various reactions occurring during the heating were evaluated by a TA Instrument simultaneous thermoanalyser SDT2960 with Al_2O_3 as reference and equipped with Al_2O_3 sample holders. The TG/DTA tests were carried out on 15 mg of dried gel specimens in N_2, from room temperature up to 1000 °C at heating rate of 10 °C min^{-1}.

The amorphous nature of the dried gels as well as the nature of any crystalline phase formed at high temperature, were ascertained by X-Ray Diffraction (XRD) using a Philips diffractometer model PW1710 (Cu Kα) at a scan rate of 1° min[-1].

^{29}Si- and ^{31}P-NMR spectra have been acquired by Direct Polarization (DP) Magic Angle Spinning (MAS) technique with a Bruker AVANCE 300 (Bruker Biospin, Milan, Italy) magnet equipped with a 4-mm wide-bore MAS probe, operating at [29]Si
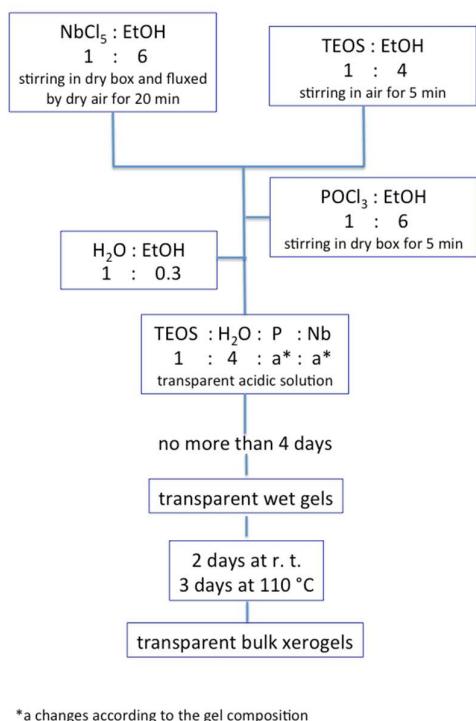
Fig. 1 Flow-chart of the synthesis procedure showing the molar ratios employed.

and ^{31}P resonating frequencies of 59.6 and 121.5 MHz, respectively. Samples have been packed in 4mm zirconia rotors with Kel-F caps and spun at 13000±1 Hz. ^{29}Si spectra consisted in 5352 acquisition points, 1000 scans, a recycle delay of 180 s and a spectral width of 400 ppm (23809 Hz), while ^{31}P spectra consisted in 2914 acquisition points, 200 scans, a recycle delay of 150 s and a spectral width of 400 ppm (48543 Hz). Only in case of ^{31}P acquisitions, a high power proton decoupling was applied by using a 30ms long TPPM15 composite pulse (-0.5 dB power attenuation) that led to signals enhancement of due to minimization of long-range proton coupling. A lower spinning speed was necessary to obtain ^{31}P spectra of 7.5NbP, 10NbP and 10NbP-500 samples.

Each spectrum was processed and elaborated by Bruker Topspin software (v.2.1). In particular, the free induction decays (FID) of ^{29}Si and ^{31}P spectra were Fourier Transformed by applying a 8 and 4 k zero filling and adopting an exponential filter function, with a line broadening of 100 and 50 Hz, respectively. Each spectrum was phase and baseline corrected.

A confocal Raman microscope (Jasco, NRS-3100) was used to obtain Raman spectra. Both the 514 nm line of an air-cooled Ar^{+} laser (Melles Griot, 35 LAP 431–220) and the 647 nm line of a water-cooled Kr^{+} laser (Coherent Innova 302C) were used. The laser line was injected into an integrated Olympus microscope and focused to a spot size of approximately 2 μm by a 100 or 20× objective. A holographic notch filter was used to reject the excitation laser line. Raman scattering was collected by a peltier-cooled 1024×128 pixel CCD photon detector (Andor DU401BVI). For most systems, it took 60 s to collect a complete data set. Fourier transform (FT) IR spectra of dried and heat treated gel samples have been obtained at room temperature by a Nicolet system, Nexus model, equipped with a DTGS KBr (deuterated triglycine sulfate with potassium bromide windows) detector. The absorption spectra were recorded in the 4000–400-cm^{-1} range with a spectral resolution of 2 cm^{-1} on samples diluted in KBr. 1.0 mg of each test sample was mixed with 200 mg of KBr in an agate mortar, and then pressed into pellets of 13 mm diameter. The spectrum of each sample represents an average of 128 scans, which were corrected for the spectrum of the blank KBr.

Results

Thermal analysis

Figure 2 shows the TG/DTA curves of the dried gels recorded in N_2 at 10 °C/min. From TG curves the same total weight loss (about 20 wt %) was evaluated for all gels and below 400 °C. Most of the weight loss was found to occur in two main steps. The first inflection point of TG curves occurs at about 80 °C and is associated with an endothermic hump in the corresponding DTA curves due to evaporation from open pores of water and alcohol physically trapped in the gels. The second inflection point of TG curves occurs at about 300 °C and in the corresponding DTA curves a second endothermic peak is seen. This peak can be related to two overlapped phenomena: the evaporation of solvent and/or organic molecules originating in the dehydration process of the gels that are more tightly trapped in the pores of the siloxane matrix, and their subsequent pyrolysis. At temperatures higher than 400 °C, no additional peaks are observed in any of the DTA curves, only a slight drift of the weight loss (about 2 wt %) still occurs on the TG curves, indicating that the elimination of organic residues as well as of any volatile species is almost completed at 400 °C. The structural evolution of dried gels upon heat treatment was studied by powder XRD as well as solid state ^{29}Si and ^{31}P NMR, Raman and IR spectroscopy within the range of temperatures used, starting from the dried gel and including gels annealed at 500 °C. This temperature stands at the minimum value at which it is possible to obtain stable and fully amorphous inorganic gel-derived materials for all studied compositions, characterized by a residual porosity of some hundreds m^2g^{-1}. The samples were prepared by slow heating at 5 °C min^{-1} to the required temperature and held at this temperature for 1 h followed by quenching.

All dried gels as well as the gels annealed at 500 °C appear amorphous, as ascertained by the analysis of XRD spectra (not reported).

ARTICLE

Journal Name
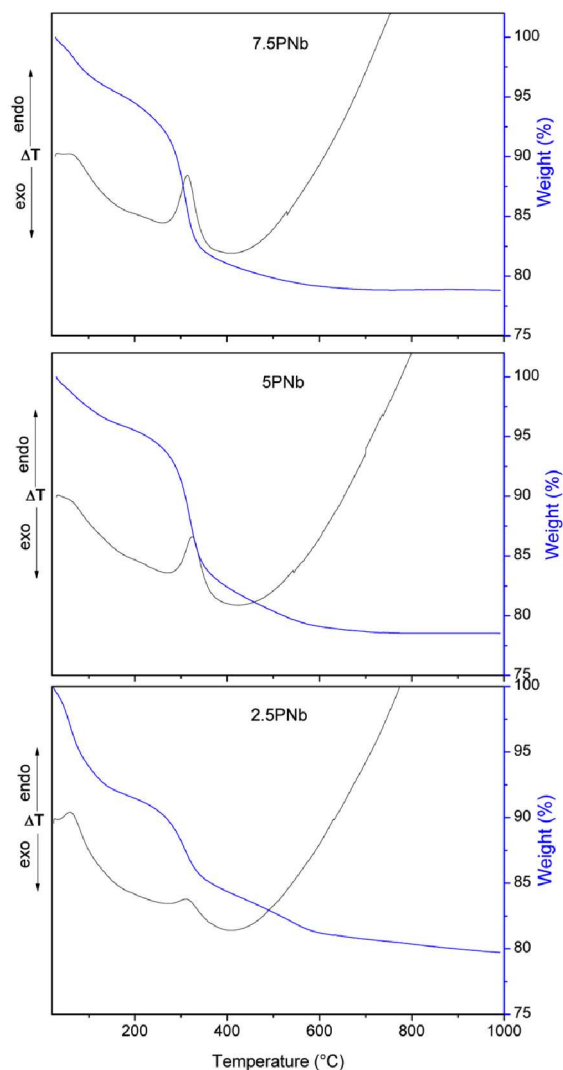

Fig.2 DTA (black line)-TG (blu line) curves of the dried gels recorded in N_2 at 10° C min^{-1}.

Table 1. Chemical shifts, δ (ppm), estimated relative intensities, I, and full width at half maximum, Fw (ppm), calculated from line fitting of the ^{29}Si resonances. Standard errors are shown in parentheses.

	dried gels			gels annealed at 500 °C		
	δ	I	Fw	δ	I	Fw
2.5 NbP	-94.5 (0.6)	0.10 (0.01)	7.1 (0.7)	-92.5 (0.8)	0.05 (0.01)	5.3 (0.7)
	-101.0 (0.04)	0.18 (0.01)	3.6 (0.1)	-101.0 (0.08)	0.25 (0.04)	5.4 (0.26)
	-109.8 (0.03)	0.72 (0.01)	6.7 (0.05)	-109.6 (0.03)	0.70 (0.01)	7.0 (0.04)
5.0 NbP	-95.4 (0.65)	0.09 (0.01)	7.2 (0.7)	-95.7 (0.77)	0.12 (0.01)	6.8 (0.60)
	-101.1 (0.11)	0.16 (0.01)	3.9 (0.07)	-100.5 (0.07)	0.09 (0.01)	4.1 (0.24)
	-109.9 (0.06)	0.75 (0.01)	6.8 (0.07)	-109.0 (0.03)	0.79 (0.01)	7.4 (0.03)
7.5 NbP	-96.2 (1.18)	0.12 (0.03)	5.9 (1.0)	-90.7 (0.08)	0.04 (0.01)	6.3 (0.7)
	-101.2 (0.17)	0.09 (0.03)	3.7 (0.4)	-99.4 (0.04)	0.15 (0.01)	5.4 (0.17)
	-109.5 (0.05)	0.78 (0.01)	7.2 (0.07)	-108.8 (0.03)	0.82 (0.01)	7.6 (0.03)
10.0 NbP	-93.9 (0.3)	0.12 (0.01)	3.9 (0.3)	-95.5 (2.5)	0.04 (0.01)	7.1 (2.0)
	-101.1 (0.03)	0.27 (0.01)	12.3 (0.07)	-100.6 (0.23)	0.06 (0.01)	5.1 (0.7)
	-110.1 (0.01)	0.61 (0.01)	5.2 (0.03)	-110.2 (0.03)	0.90 (0.01)	8.2 (0.05)

Resonance assignments: -90.0 to -95.0 ppm: Q_2 $Si(OSi)_2(OH)_2$; -100.0 to -103.0 ppm: Q_3 $Si(OSi)_3(OH)$, Q_2 $Si(OSi)(OH)_2(OX)$ with X=Nb, P; -109.0 to -112.0 ppm: Q_4 $Si(OSi)_4$, Q_3 $Si(OSi)_2(OX)(OH)$ with X=Nb, P; -112.0 to -120.0 ppm: Q_4 $Si(OSi)_{4-x}(OP)_x$ with x=1-3.

Solid state NMR

Curve fitting of the ^{29}Si and ^{31}P NMR spectra was used to determine the relative proportions of the different silicon and phosphorus network elements. Gaussian functions were used to represent the lineshapes and the resulting contributions are shown in Tables 1 and 2 for the silicon and phosphorus respectively. In the fitting procedure, the number of gaussian functions used to represent the spectra was increased until the χ^2 values were statistically significant. Errors in the relative proportions are of the order of ± 0.03. A complication is that the gaussian function centred at a particular chemical shift may not represent a single connectivity but a combination, for example $Si(OSi)_4$ and $Si(OSi)_2(OP)(OH)$. Cross linking in the ^{29}Si and ^{31}P NMR spectra can be denoted by the Q_N and Q'_N notation where Q_N indicates $Si(OSi)_N(OH)_{4-N}$ and Q'_N stands for $OP(OP)_N(OH)_{3-N}$.

All the samples, dried and after heating to 500 ºC, exhibit three resonances in their ^{29}Si NMR spectra at ca. -95, -101 and -109 ppm as illustrated in Figure 3. These can be assigned to Q_2, Q_3 and Q_4 connectivities respectively.[29] In broad terms the relative proportions of the different network elements are similar though there is some evidence for a greater variability at the highest levels of P and Nb. Also there is a tendency for the Q_4 fraction to increase with heating to 500 ºC. However within the context of the changes observed for other SiO_2-Nb_2O_5 systems the spectra changes seen here are rather small in terms of the fractions, chemical shifts and resonance linewidths.

Table 2. Chemical shifts, δ (ppm), estimated relative intensities, I, and full width at half maximum, Fw (ppm), calculated from line fitting of the ^{31}P resonances. Standard errors are shown in parentheses.

	dried gels			gels annealed at 500 °C		
	δ	I	Fw	δ	I	Fw
2.5 NbP	0.15 (0.01)	0.03 (0.001)	0.4 (0.01)	0.04 (0.05)	0.01 (0.001)	2.6 (0.14)
	-1.7 (0.02)	0.19 (0.01)	3.3 (0.09)	-	-	-
	-6.6 (0.24)	0.27 (0.03)	6.4 (0.37)	-8.9 (0.15)	0.46 (0.01)	8.8 (0.14)
	-13.0 (0.25)	0.51 (0.02)	12.0 (0.16)	-21.1 (0.11)	0.43 (0.01)	8.5 (0.25)
	-	-	-	-35.1 (0.25)	0.10 (0.01)	7.8 (0.25)
5.0 NbP	0.15 (0.01)	0.01 (0.001)	0.5 (0.02)	0.15 (0.01)	0.01 (0.001)	1.1 (0.11)
	-3.9 (0.10)	0.14 (0.03)	5.2 (0.27)	-6.6 (0.09)	0.16 (0.02)	6.6 (0.09)
	-10.5 (0.34)	0.40 (0.06)	8.2 (0.71)	-	-	-
	-18.2 (0.83)	0.46 (0.06)	12.2 (0.45)	-17.0 (0.26)	0.73 (0.02)	11.4 (0.32)
	-	-	-	-30.7 (0.71)	0.10 (0.02)	9.3 (0.55)
7.5 NbP	-	-	-	-	-	-
	-5.7 (0.19)	0.15 (0.04)	6.4 (0.26)	-	-	-
	-12.9 (0.50)	0.43 (0.06)	9.0 (0.77)	-13.7 (0.53)	0.22 (0.06)	10.6 (0.42)
	-21.8 (0.56)	0.42 (0.03)	11.8 (0.28)	-22.5 (0.65)	0.78 (0.06)	9.9 (0.44)
	-	-	-	-	-	-
10.0 NbP	-0.07 (0.01)	0.05 (0.001)	1.5 (0.03)	-	-	-
	-6.85 (0.02)	0.86 (0.01)	6.9 (0.04)	-	-	-
	-16.4 (0.10)	0.09 (0.01)	5.5 (0.13)	-13.5 (0.54)	0.25 (0.06)	10.4 (0.42)
	-	-	-	-23.2 (0.65)	0.75 (0.06)	12.7 (0.40)

Resonance assignments: 0.00 to 0.15 ppm: Q'_0 OP(OH)$_3$; -1.7 to -8.9 ppm: Q'_1 OP(OX)(OH)$_2$ with X=P, Nb; -10.5 to -22.5 ppm: Q'_2 OP(OX)$_2$(OH) with X=P, Nb; -23.5 to -35.1 ppm: Q'_3 (OP)$_{3-x}$(OX)$_x$ with x=1-2 and X=Nb, P.
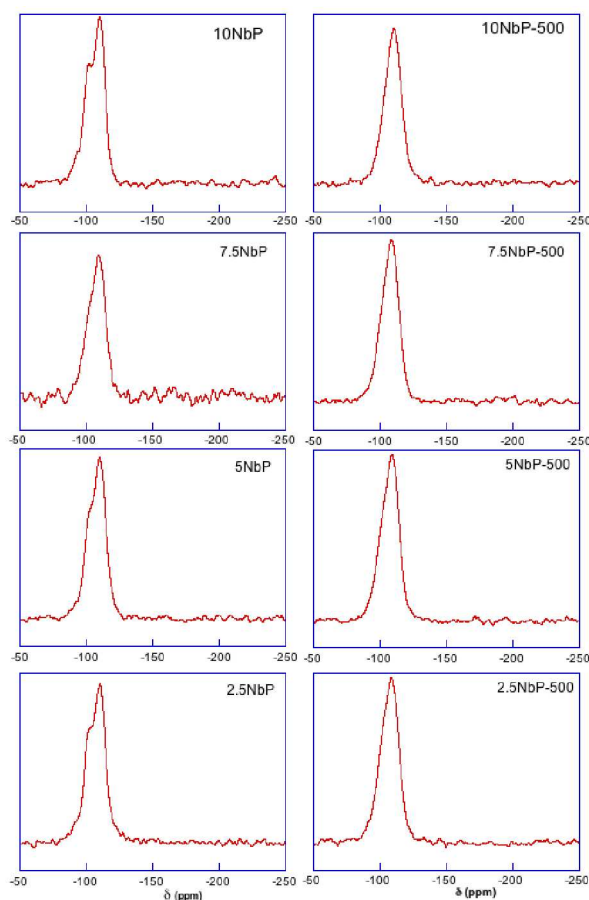
Fig.3 ^{29}Si MAS NMR spectra of the dried gels (left column) and of gels heat-treated at 500 °C for 1 h (right column).

Unlike previous phosphosilicate samples[29] the ^{31}P NMR spectra of the current materials are characterised by broad featureless resonances, centred around -20 ppm (see Figure 4). One similarity though is the presence of a sharp resonance around 0 ppm in the ^{31}P NMR spectra of the 2.5NbP and 5 NbP dried gels, typical of isolated PO$_4$ groups.[29] At the same time the 7.5 NbP dried gel shows a distinct skewing of the broad resonance towards 0 ppm. In the dried samples resonances typical of P—O—P connectivity would be seen at ca. -10 ppm (Q'_1) and -20 ppm (Q'_2) with a systematic decrease in the chemical shifts to more negative values as the amount of niobium and phosphorus increases. Owing to the broad dispersion of chemical shifts seen in the ^{31}P NMR spectra it is not possible to be definitive about the presence or otherwise of Si—O—P connectivity. Clearly resonances are seen with chemical shift ranges which overlap those which might be expected for such linkages. The strongest evidence for the absence of these groups is to be found in the stability of the ^{31}P NMR spectra of the dried samples to atmospheric moisture. Weaker supporting evidence is given the ^{29}Si chemical shifts for the highest 10 NbP content which show no evidence for a shielding one expect to see if Si—O—P bonds had been formed. The resonances seen around -5 ppm and between

-10 and -15 ppm are, however, atypical of binary phosphosilicates.[30] Although a precise assignment of these resonances is not possible, their absence from the binary phosphosilicates and presence when niobium is a reactant is strongly suggestive of the formation of P—O—Nb bonds. Two lines of argument support for this assignment. First, for a series of zirconium/phosphate environments $P(OZr)_{4-N}(OH)_N$ a stepwise decrease in chemical shift is seen with -27.4, -18.7 and -9.7 ppm for N = 0, 1 and 2 respectively,[31] while a $P(ONb)_4$[32] environment in $NbOPO_4$ gives a chemical
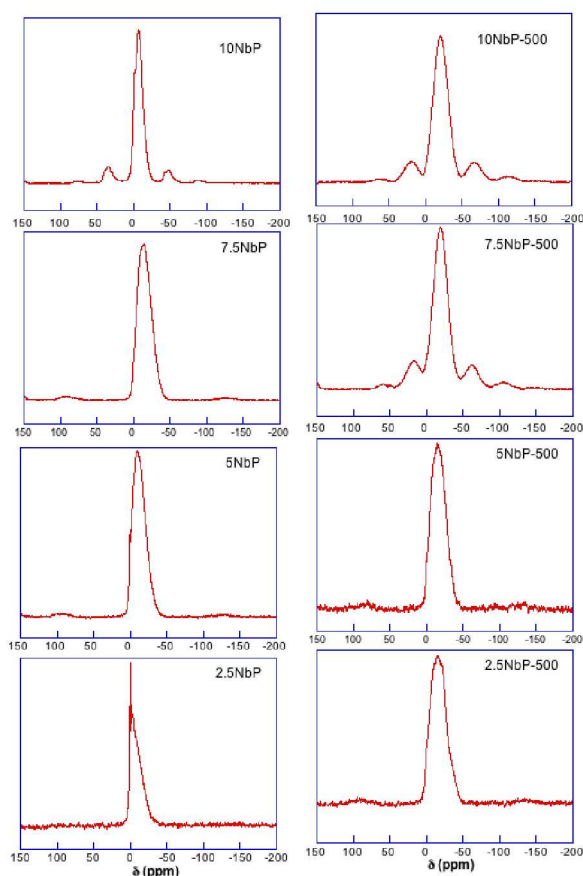

Fig.4 ^{31}P MAS NMR spectra of the dried gels (left column) and of gels heat-treated at 500 °C for 1 h (right column). The resonance lying outside 5 to -50 ppm are spinning sidebands.

shift of -24.5 ppm[33] thus it is reasonable to suppose a $P(ONb)_2(OH)_2$ environment would have a chemical shift around –6 ppm. Second, siliconiobates immersed in phosphoric acid solutions give an intense resonance in ^{31}P MAS NMR spectrum at –3 ppm and this has been assigned to $(OH)_2P(O)—O—Nb$ bonds.[34] Moreover, the ^{31}P NMR data shown in Figure 4 III(a) of the reference 34 are similar in character to the as dried samples here. Upon heating to 500 °C the resonance at 0 ppm broadens consistent with the

reduction in the mobility of the isolated PO_4 groups. A marked change is also seen in the chemical shifts towards more negative values indicative of an increased connectivity of the phosphorus. However, it is unclear whether the increased phosphorus connectivity involves the formation of bonds with phosphorus, the silicon network or niobium. Owing to the relatively small amounts of phosphorus and niobium added and the lack of resolution in the ^{29}Si NMR spectra it would not be possible to observe the expected changes in the ^{29}Si chemical shifts should Si—O—P or Si—O—Nb bonds be formed. Further insight into the origin of the changes in network connectivity was found from the ^{31}P MAS NMR data of the samples heated to 500°C but left exposed to atmospheric humidity for an extended period. After exposure it was observed that the ^{31}P NMR spectra returned to the form seen for the as dried samples suggesting the increased connectivity caused by the heat treatment arose because of the formation of Si—O—P bonds which were readily hydrolysed, rather like earlier silicophosphate materials. Despite this it must be stressed that the as dried samples showed no evidence for any hydrolysis upon exposure to atmospheric moisture further substantiating the view the phosphorus has been stabilised by the formation of P—O—Nb bonds.

Raman and Infrared spectroscopy

Broad bands are seen in the Raman spectra of dried gels (Figure 5a) and of gels annealed at 500 °C (Figure 5b) as usually occurs for amorphous samples.

Before discussing these spectra, it should be underlined that Raman bands associated with the Si–O vibrations could be masked by the Nb–O bands because the polarizability of the Nb–O bond is higher than that of the Si–O bond,[35] even if this effect is partially counteracted by the Si/Nb molar ratio, that is at least equal to 4 for the studied samples. Nevertheless, although some bending modes of Nb–O and P–O bonds which occur in 400-620 cm^{-1} range partially overlap the vibrational modes of siloxane network, the Raman bands seen in this range can be related to the latter as a consequence of the high Si/X (X = Nb or P) molar ratio.

Similarly, the overlapped stretching modes of Si–O and P–O bonds occurring in the 1000-1200 cm^{-1} region are characterized by very different relative intensities, those associated with P–O bonds being higher.[36] The above considerations, together with the lack of Raman bands related to Nb–O bonds at frequencies higher than 950 cm^{-1},[37] allows to divide the explored frequency range into three main regions: 1) 400-600 cm^{-1}, active vibrational modes of the siloxane network; 2) 600-950 cm^{-1}, active stretching modes of Nb–O bonds belonging to NbO_4 tetrahedra and/or NbO_6 octahedra; 3) 1000-1300 cm^{-1} active vibrational modes of phosphate units having different number of bridging oxygen atoms (Q'_N).

The typical Raman bands related to vibrational mode of siloxane network can be seen for all dried gels: 430 cm^{-1} ($\delta_{Si-O-Si}$), D1 (490 cm^{-1}) and D2 (610 cm^{-1}) defect bands, that are related to symmetric stretching modes of Si–O–Si bridges in regular fourfold and planar threefold rings of SiO_4 tetrahedra, respectively.[38-39] Raman bands related to vibrational modes of Nb—O and P—O bonds start to appear and develop at around 790 cm^{-1} (ν_{Nb-O} of NbO_4 tetrahedra), 880 cm^{-1} (ν_{Nb-O} of distorted NbO_6 octahedra), 935 cm^{-1}

band at 1296 cm^{-1} and the wide band lying in the 1020-1120 cm^{-1} range with features at 1050, 1080 and 1100 cm^{-1}(Figure 5b).
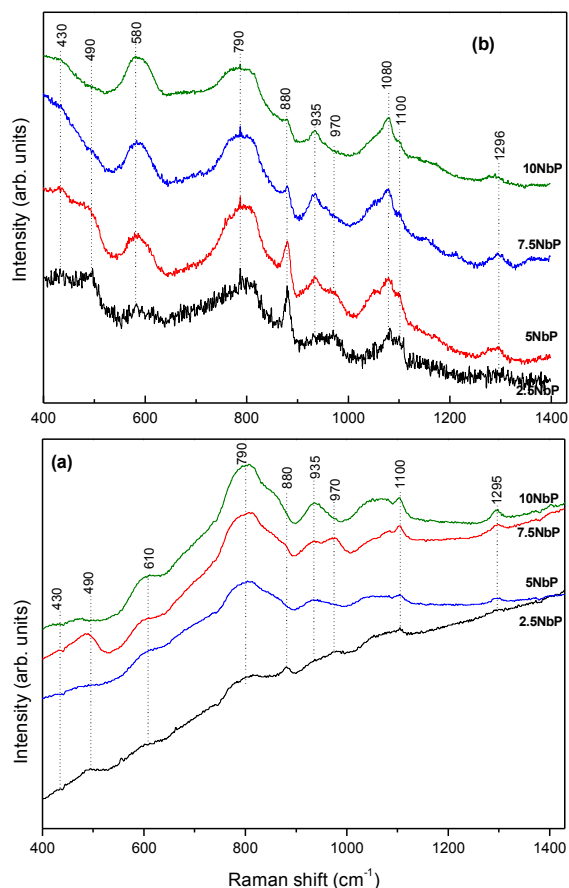

Fig. 5 Raman spectra recorded at room temperature of (a) dried gels; (b) gel samples heat-treated for 1h at 500 °C.

($\nu_{Nb=O}$ of NbO_4 tetrahedra) and 1100 cm^{-1} (ν_{P-O} of Q'_1 units).[23, 35, 36, 40] Finally, a band at 1296 cm^{-1} (ν_{P-O} of Q'_2 units) is seen,[40] that becomes more evident with decreasing the Si content, with features at 970 (ν_{Si-OH}),[23] 1050 and 1080 cm^{-1} (Figure 5a). These latter features can be related to ν_{P-O} of Q'_1 units sharing corners with diverse structural units: NbO_4 tetrahedra, NbO_6 octahedra and SiO_4 tetrahedra.

The following trends, with increasing niobium and phosphorus content, are clearly visible in the Raman spectra of samples annealed at 500 °C: (a) an increase in the intensity of the bands at about 580 cm^{-1} (ν_{Nb-O} of less distorted NbO_6 octahedra)[23, 35] and 935 cm^{-1}; (b) a decrease in the Raman bands at about 880 and 970 cm^{-1}; (c) almost no change for the largest Raman band at about 790 cm^{-1}, the
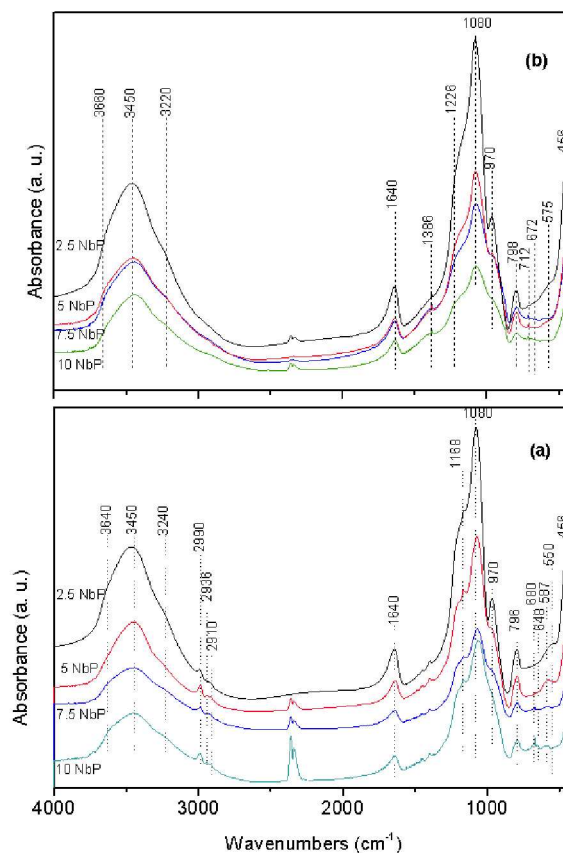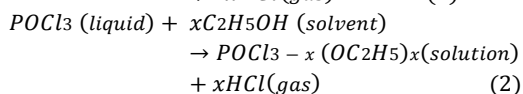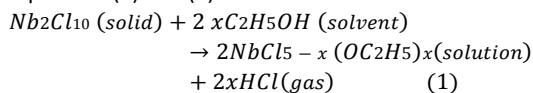

Fig. 6 FTIR spectra recorded at room temperature of (a) dried gels; (b) gel samples heat-treated for 1h at 500 °C.

FTIR spectra of dried gels and of gels annealed at 500 °C for 1 h are shown in Figure 6a and 6b, respectively. As expected, the analysis of these data provides detailed information about both the siloxane backbone structure and the hydroxyl groups' distribution. The FTIR spectra of dried gels show the main envelope in the 1000-1300 cm^{-1} region, where some of the vibration modes of partially hydrolyzed TEOS molecules (1168 and 1082 cm^{-1}) overlap the ones typical of a siloxane network (1080 and 1250 cm^{-1}) as well as the stretching modes of the phosphate (Q'_0 980-1020 cm^{-1}) and (Q'_1 1080-1160 cm^{-1} and 1020-1030 cm^{-1}) groups.[10, 41] Absorption bands at about 450 cm^{-1} ($\delta_{Si-O-Si}$) and 800 cm^{-1} (ν_s $_{P-O-P}$ and ν_s $_{Si-O-Si}$) [10, 42] are also seen. Features at 2990, 2936 and 2910 cm^{-1} (C–H stretching of methyl and methylene groups, ν_{C-H})[41] confirm the presence of coordinated alkoxo or alcohol species, while the IR bands between 580 and 680 cm^{-1} are related to Nb–O stretching of NbO_6 octahedra coupled with the bending vibrations of PO_4 groups.[37] Moreover, all dried gels exhibit a broad absorption band in the range 3000-3750 cm^{-1} centred at

about 3450 cm^{-1} with two shoulders at about 3640 and 3240 cm^{-1}. This broad band arises from O–H stretches (ν_{O-H}) involved in hydrogen bonding, while the shoulders at 3640 and 3240 cm^{-1} are related to free and strongly H-bonded OH groups, respectively.[11, 41] In fact, the hydrogen bonding causes low-frequency shifts, whose magnitude is related to the strength of hydrogen bonds in which the OH groups are involved.[11] Other O—H related bands occur at 1640 cm^{-1} (deformation modes of O–H bonds and of molecularly adsorbed water, δ_{O-H}), 970 cm^{-1} (stretching of Si—OH bonds, ν_{Si-OH}) and 550 cm^{-1} (bending of Si—OH bonds, δ_{Si-OH}).[42] Finally, all FTIR spectra of dried gels show features in the range 580-680 cm^{-1}, that appear more evident with decreasing Si content, arising from overlapping modes of ν_{Nb-O} of NbO$_6$ octahedra and ν_s $_{P-O-P}$ of PO$_4$ tetrahedra.[37, 43]
The analysis of the FTIR spectra of gel-derived samples annealed at 500 °C for 1 h (Figure 6b) show that the structural evolution of the dried gels upon heating results in absorption bands characteristic of a mixed framework of SiO$_4$ and PO$_4$ tetrahedra with NbO$_6$ octahedra: 1386 cm^{-1} (P=O bond stretch)[42], shoulder at about 1226 cm^{-1} (Si—O bond stretch in Q$_4$ units)[41] and 1080 cm^{-1} (combination of P—O stretches of the P—O—P and P—O—Si bridging units)[42]. An unexpected result is the presence in these FTIR spectra of evident OH related bands that appear almost unchanged with respect to those occurring for dried gels. Particularly, the δ_{O-H} band indicates that the annealed samples adsorb water during the cooling. Small changes are seen for the shoulders of ν_{O-H} band: the former shifts to about 3660 cm^{-1}, the latter shifts to 3220 cm^{-1} (Figure 6b).

Discussion

The synthesis of chemical gels in a multi-component system requires molecular precursors with comparable hydrolysis rates in order to promote cross-linking between clusters of different components with similar size, thereby encouraging gelation instead of precipitation and/or co-precipitation. However, in the present system both NbCl$_5$ (from the dimeric solid Nb$_2$Cl$_{10}$)[44], and POCl$_3$ are more reactive that TEOS consequently the precise nature of the hydrolysis step is of key importance in the overall procedure. Thus, niobium ions, Nb^{5+}, in aqueous environments undergo rapid hydrolysis giving rise to a precipitate of hydrated niobium pentoxide, Nb$_2$O$_5$·nH$_2$O.[23] While studies of binary SiO$_2$-P$_2$O$_5$ dried gels have only shown the formation of P-hydrolyzed species[10, 29], such as H$_3$PO$_4$ and H$_4$P$_2$O$_7$ because of the instability of the P—O—Si bonds towards the hydrolysis in an acidic aqueous environment.
The high moisture sensitivity of Nb$_2$Cl$_{10}$ and POCl$_3$ was controlled by dissolving them in absolute ethanol, according to equations (1) and (2):

$$Nb_2Cl_{10} \ (solid) + 2 \ xC_2H_5OH \ (solvent)$$
$$\rightarrow 2NbCl_{5-x} \ (OC_2H_5)_x (solution)$$
$$+ 2xHCl(gas) \qquad (1)$$
$$POCl_3 \ (liquid) + \ xC_2H_5OH \ (solvent)$$
$$\rightarrow POCl_{3-x} \ (OC_2H_5)_x (solution)$$
$$+ xHCl(gas) \qquad (2)$$

The partially, POCl$_{3-x}$(OC$_2$H$_5$)$_x$, or completely, PO(OC$_2$H$_5$)$_3$, substituted phosphoryl chloride species are formed by the strongly exothermic reaction (2). HCl stripping was performed by dry air bubbling to control the degree of conversion of the reaction (1). Consequently, partially, NbCl$_{5-x}$(OC$_2$H$_5$)$_x$, or completely, Nb(OC$_2$H$_5$)$_5$, substituted species were formed. A stripping time of 20 min was used both to avoid the complete substitution and to preserve, to some extent, unreacted molecules of Nb$_2$Cl$_{10}$ in solution. These molecules are thought to play an important role in the stabilization of the niobium ions in aqueous solution toward the precipitation of Nb$_2$O$_5$·nH$_2$O by the creation of species such as Nb(OH)$_2$Cl$_4^-$ and Nb(OH)$_2$Cl$_3$ at low HCl concentrations[45] or NbOCl$_5^{2-}$ and NbCl$_6^-$ complexes in aqueous saturated HCl solution of niobium pentachloride[46]. As a consequence of carrying out these premixing reactions with ethanol, no precipitation was observed when the final solution was obtained by mixing the alcoholic solution of the precursors with the hydroalcoholic one (Figure 1). Nevertheless, several species that can be hydrolysed are present in the final solution: niobium oxo-hydroxo-chloro complexes, phosphorus chloro-ethoxide species and TEOS. Among them, TEOS should be the least reactive species, as the silicon exhibit the lower positive partial charge.[47] Consequently, the hydrolysis will begin with the niobium oxo-hydroxo-chloro complexes and phosphorus chloro-ethoxide species forming Nb and P hydroxo and oxo soluble oligomers. Clear evidence for the formation of Nb—O—P bonds being provided by the ^{31}P NMR data. Whilst these reactions are taking place the TEOS hydrolysis will start to occur at a significant rate offering the possibility of both self- and cross-condensation which may hinder the further self-condensation of P and Nb oxo oligomers. However, as the siloxane network develops, it is unclear whether any cross-linking with the Nb oligomeric species actually occurs. Indeed the close similarity seen for the ^{29}Si NMR spectra of the various dried materials might suggest the general silicon network created is unperturbed by the presence of either phosphorus or niobium. Such a conclusion would be consistent with previous work on other SiO$_2$-Nb$_2$O$_5$ systems.[27] Notwithstanding the similarity in the ^{29}Si NMR spectra, there is still uncertainty since whatever cross-linking takes place with the Nb oligomers and siloxane must arise by Nb—O—Si bonds because of the instability of the P—O—Si bonds while the substituent effect of Nb on ^{29}Si chemical shifts is not well established. What little evidence there is on the effect of Nb on the ^{29}Si chemical shift[27] suggests it might be small and consequently would not affect the resonance positions, in contrast to the significant changes seen with P incorporation into a siloxane network[29]. Thus the ^{29}Si NMR data are plausibly consistent with some Nb—O—Si cross-linking. Unlike the previous work[27] the extent of silicon cross-linking in the dried materials is significantly greater but affected far less by heating. Thus with the dried 2.5NbP 72% of the silicon is present as Q^4 units whereas it is only 50% in reference 27. On the other hand after heating to 500°C the Q^4 in the present materials has only increased to 80%, similar to the 79%[27]. Consequently it appears that a more heavily cross-linked matrix is initially formed which is

more stable to further dehydroxylation. The most plausible explanation for this increase in Q^4 is the formation of Si—O—Nb bonds particularly as the Q^4 fraction increases with Nb/P content. At the same time the absence of any change in the Q^4 chemical shift is consistent with the very small effect of niobium on the [29]Si chemical shift. The NMR data is therefore consistent with the preferential reaction between silicon and niobium on the one hand and niobium and phosphorus on the other with the niobium serving to anchor the phosphorus into the silicon network with a less hydrolytically labile linkage. Annealing at 500°C causes marked increases in the phosphorus connectivity as witnessed by the shielding effects seen in the ^{31}P NMR spectra. However, it is difficult to be definitive about the chemical changes giving rise to these shielding effects since the resonances are broad and so represent a range of different environments while the chemical shift ranges would be consistent with various phosphorus connectivities $Q'_N(Si,P,Nb)$. Nevertheless, there is evidence the annealing causes the formation of labile bonds since prolonged exposure to atmospheric humidity results in a deshielding in the ^{31}P NMR spectrum indicating a return to the connectivity seen in the initially prepared dried gels. Significantly though the prolonged exposure to the atmospheric moisture did not reduce the phosphorus connectivity of the dried gels and hence the stabilisation of the phosphorus in the network through the use of niobium. Thus allowing their storage and manipulation without special attention. In the light of the lability of the bonds formed by annealing it is plausible this process introduces Si—O—P cross-linking.

The Raman and IR analysis also agrees with the above interpretation. Raman spectra of both dried and annealed gels give a clear evidence for the presence of Nb—O—X (X=Si and/or P) as well as of NbO_4 tetrahedra. Particularly, the large band at about 580 cm^{-1} in the Raman spectra of annealed gels (Figure 5b) indicates the presence of clustering of NbO_6 octahedra containing Nb—O—X (X=Si and/or P) bridges, as Nb—O stretch belonging to nanodomains formed by clusters of corner-sharing NbO_6 octahedra should occur at higher frequency.[35] The stabilization of the four-fold coordination of Nb^{5+} plays a key role in realizing the interconnected network in which the cross-condensation between Nb- and P-units allows the formation of Nb—O—X (X=Si and/or P) and P—O—X (X=Nb and/or P) bridges. Six-fold coordination of Nb^{5+} is usually the most commonly seen, since Nb^{5+} is too large a size to fit into an oxygen-anion tetrahedron.[48] Nonetheless, Nb^{5+} has been found in four-fold coordination in some rare-earth $ANbO_4$ (A=Y, Sm and La) crystalline compounds[48] as well as in gel-derived niobium-silicon mixed-oxides[23]. In this latter case the stabilization was obtained in amorphous samples with a high Si content (at least 90 atom%) as a consequence of the high dispersion of the niobium into a framework of SiO_4 tetrahedra.[23] But in the Nb-P-Si case, contrary to what occurs in binary gel-derived niobium-silicon mixed oxide,[23] the NbO_4 → NbO_6 transformation does not take place with increasing niobium content, whereas the transformation of distorted NbO_6 octahedra into less distorted NbO_6 ones happens. The increase of less distorted NbO_6 octahedra facilitates the

formation of Nb—O—X (X=Si and/or P) bridges so hindering the segregation of a niobium rich phase even in the gel-derived sample with the highest niobium and phosphorus content.

The lack of bands related to alkyl groups in the FTIR spectra of the annealed gels confirms that the annealing results in the complete removal of organic residuals. Consequently the similarity of the FTIR spectra for the dried and annealed gels in the region corresponding to the O—H related bands must be indicative of the inorganic OH and absorbed water rather than any residual organic component. According with the solid state NMR analysis, the siloxane network of dried gels exhibit an unusual high polymerization degree that is only slightly increased by the heat treatment at 500 °C. Therefore, during the heat treatment polycondensation reactions occur mainly involving Nb- and P-oxygen polyhedra, whose excess negative charge must be balanced by H atoms due to the lack of metallic cations, forming a porous mixed Nb-P-Si framework, characterized by the presence of different kinds of OH groups: Si—OH, Nb—OH and P—OH. The presence of P=O and Nb=O double bonds leads to the formation of stronger hydrogen bonds while free hydroxyl groups are mainly Si—OH bonds. The presence of a broad band around 3450 cm^{-1} for the annealed samples shows that the annealed gels, besides the Lewis acid sites, continue to keep a wide distribution of Brønsted acid sites of different strength as found in heat treated mesoporous niobium-phosphate[19] and in Nb_2O_5-SiO_2 gel-derived samples modified by phosphoric acid,[34] making the synthesized materials a good candidate to act as solid acid for heterogeneous catalysis.

Conclusions

For the first time amorphous niobium-phosphorus-silicon mixed oxide materials, with molar ratio P/Nb=1 and Si content ranging from 95 to 80 mol%, have been obtained by an innovative sol-gel procedure wholly performed at room temperature. In this procedure the very different reactivity of TEOS with respect to that of the other precursors, Nb_2Cl_{10} and $POCl_3$, was controlled by a reacting the latter two with ethanol to give niobium oxo-hydroxo-chloro complexes and phosphorus chloro-ethoxide species prior to mixing with TEOS, rather than by prehydrolysis of the TEOS. The niobium and phosphorus species then react to form Nb oligomeric species which act both as cross-linking reagents and as catalysts for the condensation reactions of siloxane oligomers. The absence of a TEOS prehydrolysis step makes the formation of a homogeneous sol easier. Dried gels formed by a siloxane framework of SiO_4 tetrahedra, in which niobium (NbO_4 and NbO_6) and phosphorus (PO_4) structural units are uniformly dispersed, were obtained from the prepared sol.

In the heat-treated gels segregation of niobium and phosphorus does not occur; on the contrary Nb—O—X (X = Si, P) bridges are formed by cross-condensation between Nb- and P-units. On increasing the niobium content, a transformation of distorted NbO_6 octahedra into ordered NbO_6 ones occurs, facilitating the cross-condensation, so hindering the

segregation even in the gel-derived sample containing the highest Nb and P content.

Finally, the presence in the heat-treated gels of OH groups exhibiting a chemical environment similar to that observed in the corresponding dried gels opens opportunities for their use as acid solids for heterogeneous catalysis.

References

1 Y. G. Jin, S. Z. Qiao, J. C. Diniz da Costa, B. J. Wood, B. P. Ladewig, G. Q. Lu, *Adv. Funct. Mater.,* 2007*, **17**, 3304-3311.*

2. J. Mosa, G. Larramona, A. Durán, M. Aparicio*, J. Membr. Sci.,* 2008*, **307**, 21-27.*

3. Y. G. Jin, S. Z. Qiao, Z. P. Xu, Z. Yan, Y. Huang, J. C. Diniz da Costa, G. Q. Lu, *J. Mater. Chem.,* 2009*, **19**, 2363-2372.*

4. Z. Di, H. Li, D. Mao, X. Chen, M. Xiao*, Fuel Cells*, 2013*, **13**, 126-133.*

5. V. G. Ponomareva, E. S. Shutova*, Inorganic Materials,* 2014*, **50**, 1056-1062.*

6. A. Tilocca, A. N. Cormak*, J. Phys. Chem. B,* 2007*, **111**, 14256-14264.*

7. D. Carta, J. C. Knowles, P. Guerry, M. E. Smith, R. J. Newport, *J. Mater. Chem.,* 2009*, **19**, 150-158.*

8. A. García, M. Colilla, I. Izquierdo-Barba, M. Vallet-Regí*, Chem. Mater.,* 2009*, **21**, 4135-4145.*

9. A. Pedone, T. Charpentier, G. Malavasi, M. C. Menziani*, Chem. Mater.,* 2010*, **22**, 5644-5652.*

10. A. Aronne, M. Turco, G. Bagnasco, P. Pernice, M. Di Serio, N. J. Clayden, E. Marenna, E. Fanelli*, Chem. Mater.,* 2005*, **17**, 2081-2090.*

11. N. J. Clayden, S. Esposito, P. Pernice, A. Aronne, J. Mater. Chem., 2002*, **12**, 3746-3753.*

12. S. Lassiaz, D. Labarre, A. Galarneau, D. Brunel, P. H. Mutin*, J. Mater. Chem.,* 2011*, **21**, 8199-8205.*

13. L. Q. Wang, W. D. Samuels, G. J. Exarhos, B. I. Lee, Z. J. Cao*, Mater. Chem.,* 1998*, **8**, 165-169.*

14. J. Goubeau, K. O. Christie, W. Teske, W. Z. Z. Wilborn*, Anorg. Allg. Chem.,* 1963*, **325**, 26-42.*

15. A. Styskalik, D. Skoda, Z. Moravec , J. G. Abbott, C. E. Barnes, J. Pinkas*, J. Microporous Mesoporous Mater.,* 2014*, **197**, 204-212.*

16. A. Matsuda, Y. Nono, K. Tadanaga, T. Minami, M. Tatsumisago*, Solid State Ionics,* 2003*, **162-163**, 253-259.*

17. T. Amaroli, G. Busca, C. Carlini, M. Giuttari, A. M. Raspolli Galletti, G. J. Sbrana*, Mol. Catal. A: Chem.,* 2000*, **151**, 233-243.*

18. P. Carniti, A. Gervasini, S. Biella, A. Auroux*, Chem. Mater.,* 2005*, **17**, 6128-6136.*

19. Y. Zhang, J. Wang, J. Ren, X. Liu, X. Li, Y. Xia, G. Lu, Y. Wang*, Catal. Sci. Technol.,* 2012*, **2**, 2485-2491.*

20. M. H. S. de la Cruz, J. F. C. da Silva, E. R. Lachter*, Catal. Today,* 2006*, **118**, 379-384.*

21. A. S. Rocha, A. M. S. Forrester, M. H. C. de la Cruz, C. T. da Silva*, Catal. Commun.,* 2008*, **9**, 1959-1965.*

22. Y. Choi, D. S. Park, H. J. Yun, J. Baek, D. Yun, J. Yi*, ChemSusChem,* 2012*, **5**, 2460-2468.*

23 A. Aronne, E. Marenna, V. Califano, E. Fanelli, P. Pernice, M. Trifuoggi, A. Vergara*, J. Sol-Gel Sci. Technol.,* 2007*, **43**, 193-204.*

24. A. Aronne, M. Turco, G. Bagnasco, G. Ramis, E. Santacesaria, M. Di Serio, E. Marenna, M. Bevilacqua, C. Cammarano, E. Fanelli*, Appl Catal A: General,* 2008*, **347**, 179-185.*

25. B. Julián, C. Gervais, E. Cordoncillo, P. Escribano, F. Babonneau, C. Sanchez*, Chem. Mater.,* 2003*, **15**, 3026-3034.*

26. B. Julián, C. Gervais, M. N. Rager, J. Maquet, E. Cordoncillo, P. Escribano, F. Babonneau, C. Sanchez*, Chem. Mater.,* 2004*, **16**, 521-529.*

27. K. O. Drake, D. Carta, L. J. Skipper, F. E. Sowrey, R. J. Newport, M. E. Smith*, Solid State NMR,* 2005*, **27**, 28-36.*

28. M. S. P. Francisco, Y. J. Gushikem*, Mater. Chem.,* 2002*, **12**, 2552-2558.*

29. N. J. Clayden, S. Esposito, P. Pernice, A. Aronne*, J. Mater. Chem.,* 2001*, **11**, 936-943.*

30. T. R. Krawietz, P. Lin, K. E. Lotterhos, P. D. Torres, D. H. Barich, A. Clearfield, J. F. Haw*, J. Am. Chem. Soc.,* 1998*, **120**, 8502-8511.*

31. N. J. Clayden*, J. Chem. Soc., Dalton Trans.,* 1987*, **32**, 1877-1881.*

32. J. M. Longo, P. Kierkegaard*, Acta Chemica Scandinavia,* 1966*, **20**, 72-78.*

33. D. R. Sørensen, U. G. Nielsen, E. M. Skou, *J. Solid State Chem.,* 2014*, **219**, 80–86.*

34. M. S. P. Francisco, W. S. Cardoso, Y. Gushikem, R. Landers, Y. V. Kholin, *Langmuir,* 2004*, **20**, 8707-8714.*

35. A. Aronne, V. N. Sigaev, B. Champagnon, E. Fanelli, V. Califano, L. Z. Usmanova, P. Pernice*, J. Non-Cryst. Solids,* 2005*, **351**, 3610-3618.*

36. C. Nelson, D. R. Tallant*, Phys. Chem. Glasses,* 1984*, **25**, 31-38.*

37. G. T. Stranford, R. A. Condrate Sr.*, J. Mater. Sci. Letters,* 1984*, **3**, 303-306.*

38. A. E. Geissberger, F. L. Galeener*, Phys. Rev. B,* 1983*, **28**, 3266-3271.*

39. C. J. Brinker, D. R. Tallant, E. P. Roth, C. S. Ashley*, J. Non-Cryst. Solids,* 1986*, **82**, 117-126.*

40. L. Zhang, K. L. Brow*, J. Am. Ceram. Soc.,* 2011*, **94**, 3123-3130.*

41. P. Innocenzi*, J. Non-Cryst. Solids*, 2003*, **316**, 309-319.*

42. M. D'Apuzzo, A. Aronne, S. Esposito, P. Pernice*, J. Sol-Gel Sci. Technol.*, 2000*, **17**, 247-254.*

43. M. J. Bushiri, R. S. Jayasree, M. Fakhfakh, V. U. Nayar*, Mater. Chem. Phys.,* 2002*, **73**, 179-185.*

44. A. Zalkin, D. E. Sands*, Acta Cryst.* 1958*, **11**, 615-619.*

45. D. Brown in *Comprehensive inorganic chemistry,* ed. J. C. Blair, H. J. Emeléus, R. Nyholm, A. F. Trotman-Dickenson, Pergamon Press Ltd., Oxford, *1973*, vol. 3, p. 587.

46. J. E. D. Davies, D. A. Long*, J. Chem. Soc. A,* 1968*, 2560-2564.*

47. J. Livage, M. Henry, C. Sanchez*, Prog. Solid State Chem.,* 1988*, **18**, 259-342.*

48. J. M. Jehng, I. E. Wachs*, Chem. Mater.,* 1991*, **3**, 100-107.*